Article

Site-Specific Labeling of Proteins with Near-IR Dyes

Chen-Ming Lin, Syed Muhammad Usama and Kevin Burgess *

    Department of Chemistry, Texas A & M University, Box 30012, College Station, TX 77842, USA

* Correspondence: burgess@tamu.edu@e-mail.com; Tel.: +1-979-845-4345

Abstract: Convenient labeling of proteins is important for observing its function under physiological conditions. In tissues particularly, heptamethine cyanine dyes (Cy-7) are valuable because they absorb in near infrared (NIR) region (750 – 900 nm) where light penetration is maximal. In this work, we found Cy-7 dyes with a *meso*-Cl functionality covalently binding to proteins with free Cys residues under physiological conditions (aqueous environments, at near neutral pH, and 37 °C). It transpired that the *meso*-Cl of the dye was displaced by free thiols in protein, while nucleophilic side-chains from amino acids like Tyr, Lys, and Ser did not react. This finding shows a new possibility for convenient and selective labeling of proteins with near-IR fluorescent probes.

Keywords: heptamethine cyanine, protein labeling, thiol labeling, cancer targeting, vimentin

---

1. Introduction

Hydrophilic near-infrared (NIR) fluorescent dyes are valued for in-depth imaging in tissue, and heptamethine cyanines, or Cy-7 dyes, which absorb in NIR region (700-900 nm), are amongst the most widely used of these [1]. Indocyanine green (ICG, Figure 1), the only FDA-approved Cy-7 dye, has been wide used in medical and clinical diagnostics [2-4].

Many applications of Cy-7 dyes require that they be covalently conjugated to, for example, antibodies, cell surface targeting peptides/biomarkers, and small molecule substrates. This is often achieved by modifying Cy-7 derivatives with coupling functionalities such as maleimide, succinimide esters, isocyanates, or sulfonyl halides. Throughout, the challenge with strategies like this is balancing the demands of experimental convenience with selectivity towards targeted amino acid types. Extensive modifications to Cy-7 dyes can also alter their solubility and photophysical properties [5].

Figure 1 shows dyes featured in this study. Probes of this type, *i.e.* with a 1-chloro-2,6-disubstituted cyclohexane (*i.e.* MHI-148, IR-780, IR-783, and DZ-1) [6-8] are known for their tumor localizing properties [9-12]. Therefore, these Cy-7 dyes are potential carriers of cytotoxic payload for combined cancer targeted therapy and imaging [13-16]. Our research in this area, we happened to make a surprising finding regarding such conjugation process. Specifically, when investigating *in vitro* reactions, and cell lysates featuring MHI-148, it was found to covalently bind to several proteins with high selectivity as evidenced by gel electrophoresis and NIR imaging at around 800 nm.

We hypothesized that the *meso*-Cl of MHI-148 was substituted by nucleophilic functional groups of amino acids (Cys, Ser, Tyr, and Lys) of proteins. This paper provides data to support this hypothesis and understand the selectivity.
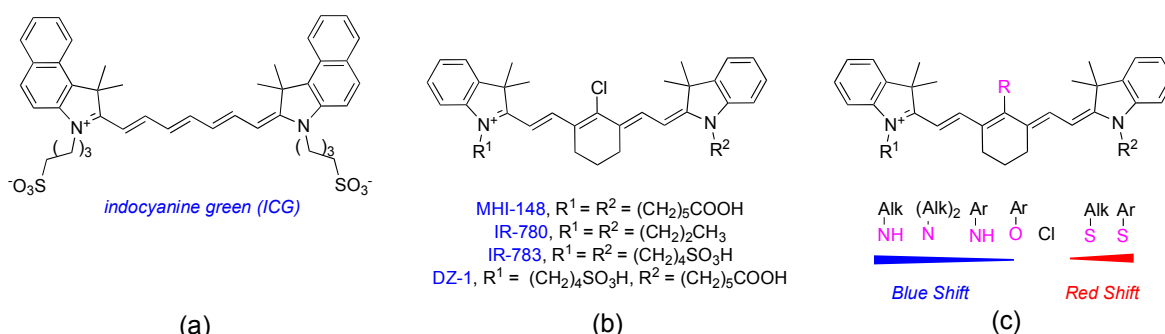
Figure 1. Structures of: (**a**) ICG; (**b**) cancer tissue targeting Cy-7 dyes and their *meso*-substituted derivatives; and, (**c**) graphical representation of the effects of *meso*-substitution on electronic spectra.

2. Results and Discussion

2.1. Syntheses Of Amino Acid Substituted Cy-7 Dyes
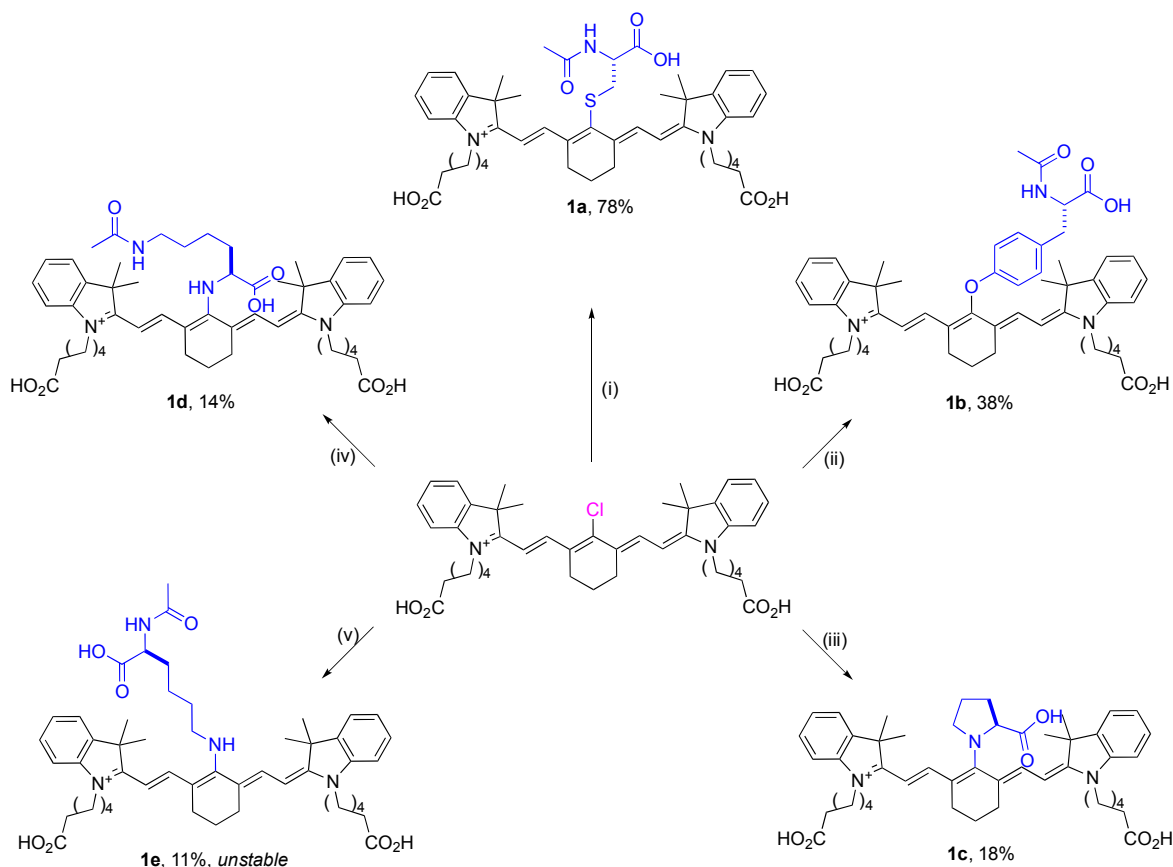
Scheme 1. Preparation of amino acid substituted Cy-7 dyes. (i) *N*-acetyl-L-cysteine (1 eq.), iPr₂NEt (1.5 eq.), DMF, 25 °C, 1 h (ii) *N*-acetyl-L-tyrosine (1 eq.), NaH, DMF, 25 °C, 18 h (iii) proline (1 eq.), iPr₂NEt (1 eq), DMF, 60 °C, 2 h (iv) Nε-acetyl-L-lysine (1 eq.), iPr₂NEt (1 eq), DMF, 60 °C, 20 h (v) *N*α-acetyl-L-lysine(1 eq.), iPr₂NEt (1 eq), DMF, 60 °C, 20 h.

Reactions under controlled conditions were used to test if nucleophilic substitution of the chloride of MHI-148 was possibly occurred e in DMF solvent. Thus, several amino acids with different nucleophilic side chains (*N*-acetyl-L-cysteine, *N*-acetyl-L-tyrosine, *N*α-acetyl-L-lysine, *N*ε-acetyl-L-lysine, and L-proline) were reacted with MHI-148 under conditions that were varied to force the reactions to proceed.   The corresponding amino-acid-substituted Cy-7 dyes were indeed formed (Scheme 1); these were isolated, characterized, and later used as standards for comparison of

58 HPLC retention times. Serine was excluded from these experiments because alcohol hydroxyl
59 groups are known to not substitute the *meso*-Cl without complications [17-20].
60   *N*-Acetyl-L-cysteine was the most reactive nucleophile of the five amino acids studied. In the
61 presence of Hünig's base, MHI-148 was completely converted to the thiol-substituted product
62 within an hour at 25 °C in DMF (0.1 M 1:1 dye:Cys-derivative, LC-MS analyses). Four other amino
63 acid nucleophiles studied required a stronger base (Tyr), and/or elevated temperatures (Pro and
64 Lys), and even then, a significant amount of unreacted MHI-148 was observed after several hours.
65 *N*α-Acetyl-L-lysine reacted faster than those three, giving the substituted product **1e,** which can be
66 isolated by reversed-phase flash chromatography; however, significant decomposition was
67 observed (color change from blue to pink) in organic solvents after only 20 min. Overall, this data
68 indicated the *meso*-Cl substitution reactivity was thiol > phenol > 2° amine > 1° amine. At this stage,
69 we did not know if these reactivities would also be observed in aqueous media, but preferential
70 conjugation of MHI-148 to Cys residues seemed more likely.

71 *2.2. Optical Properties Of Amino Acid Substituted Cy-7 Dyes*

72   Figure 2 shows absorbance and fluorescence of compounds **1a-d** in 10 mM PBS buffer. The *S*-
73 or *O*-substituted compounds (**1a** and **1b**) had absorbance and fluorescence spectra similar to those of
74 MHI-148. Significant red-shifts of absorbance and fluorescence were observed for both
75 *N*-substituted Cy-7 dyes (**1c** and **1d**), which have been attributed [21,22] to conjugation of the
76 nitrogen lone pair with the Cy-7 core. Interestingly, the peaks for the *N*-substituted products are
77 significantly broader implying more vibrational fine structures than the *S*- or *O*-substituted products
78 [23].
79

80
81   (**a**)   (**b**)

82
83   (**c**)   (**d**)
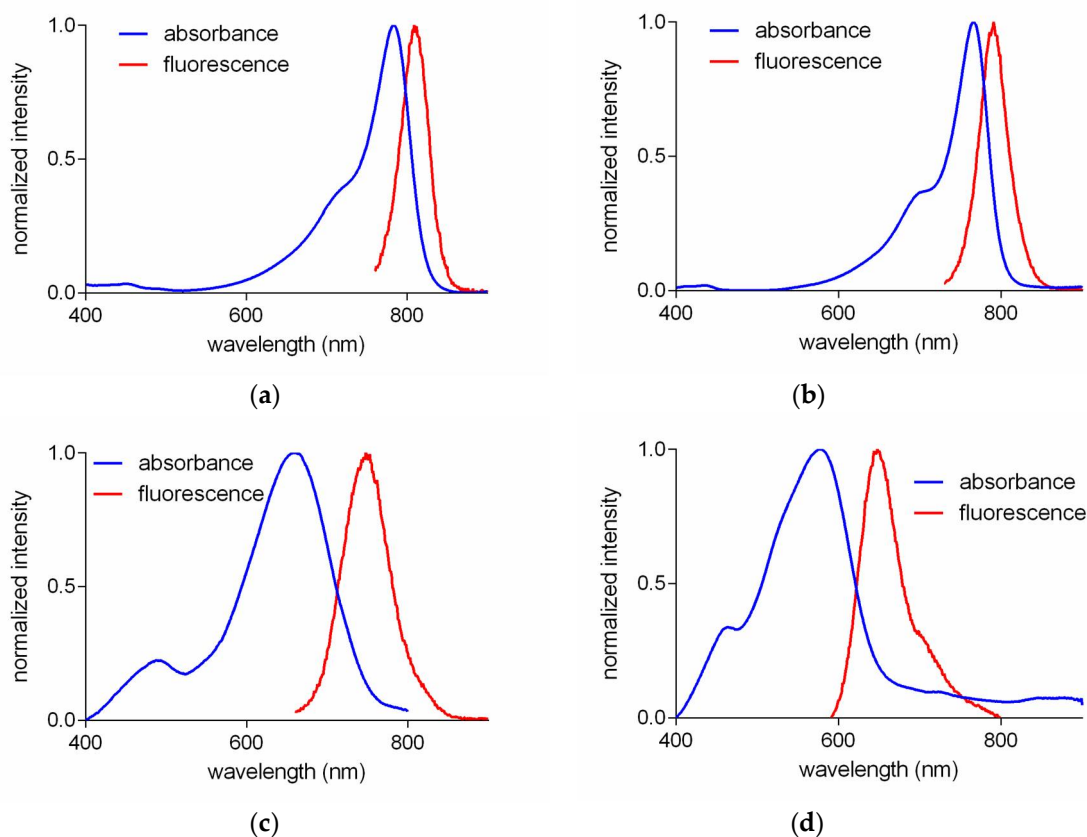
84   **Figure 2.** Normalized absorbance and fluorescence of compounds **1a-d** in pH 7.24 10 mM PBS buffer.
85   (**a**) compound **1a**: $\lambda_{max\ abs}$ 783 nm, $\lambda_{max\ emiss}$ 809 nm. (**b**) compound **1b**: $\lambda_{max\ abs}$ 766 nm, $\lambda_{max\ emiss}$ 791 nm.
86   (**c**) compound **1c**: $\lambda_{max\ abs}$ 658 nm, $\lambda_{max\ emiss}$ 748 nm. (**d**) compound **1d**: $\lambda_{max\ abs}$ 578 nm, $\lambda_{max\ emiss}$ 648 nm.

87

88   *2.3. meso-Cl Functionality of Cy-7 Dyes Is Essential For Cys-selective Protein Labeling*

89   Vimentin, a structural protein, was chosen for study because it has only one Cys residue (C328).
90   Vimentin (1 μg, 1 μM) was incubated with Cy-7 dyes containing *meso*-Cl (MHI-148, IR-780, IR-783,
91   and DZ-1; 10 μM) and with Cy-7 dyes without *meso*-Cl (ICG and **1a**) for comparison (throughout, 10
92   μM in 50 mM pH 7.24 HEPES buffer at 37 °C for up to 24 h).   Equal amount of the samples (100 ng)
93   were electrophoresed under reducing conditions, and the gel was analyzed using a NIR imager.
94   Only the Cy-7 dyes containing *meso*-Cl reacted to give a band observable at 800 nm   (Figure 3).
95

(a)   (b)
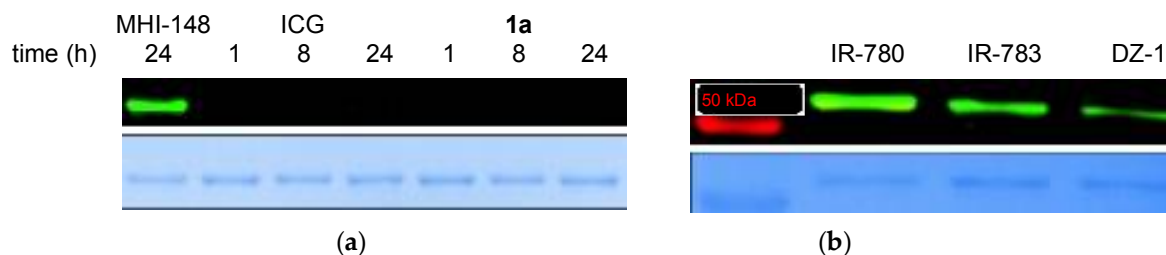
Figure 3. NIR-fluorescent gel image of (**a**) vimentin (1 μM) incubated with different cyanines (10 μM)
in 50 mM pH 7.24 HEPES buffer at different incubation time; (**b**) vimentin (1 μM) incubated with
IR-780, IR-783, and DZ-1 in the same buffer as (**a**) for 24 h. CBB-G250 staining indicated equal
amount of protein (100 ng) was loaded into gel.

102   Further evidence for the superior reactivities of Cys side-chains over other nucleophilic amino
103   acid residues was obtained via competition experiments.   Thus, MHI-148 (200 μM) in 50 mM pH 8.0
104   HEPES buffer was incubated with equimolecular amounts of five amino acids (Scheme 2) at 37 °C,
105   and the reaction was monitored by HPLC up to 27 h.   Prototypes of this experiment were intended
106   to measure relative rates, however, only formation of the Cys-product **1a** occurred (HPLC spike with
107   the standard from Scheme 1 {Figure 4}, and LC-MS analyses).   Under these conditions
108   approximately 32% of MHI-148 was substituted and 68% remained after 15 h.   This observation
109   implied amine, alcohol, and phenol side-chains in the protein did not react with the dye.
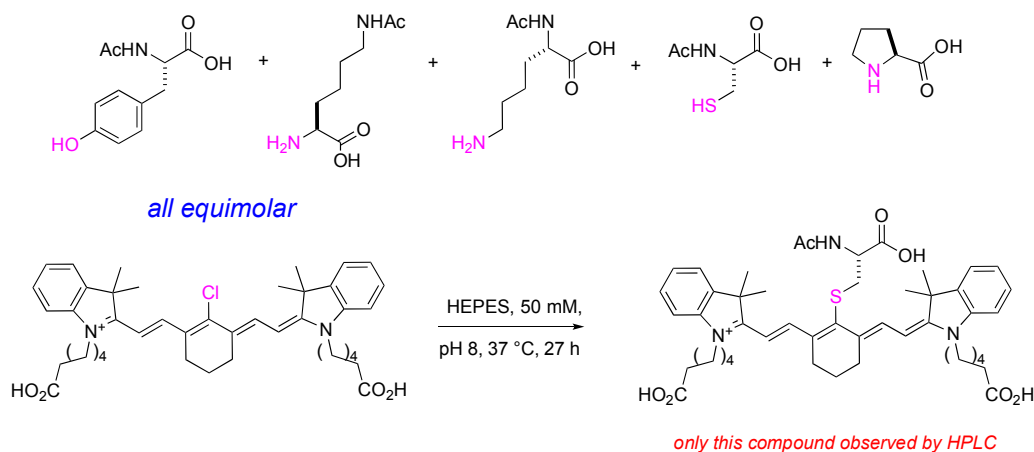
111   **Scheme 2.** Competition study of MHI-148 with amino acids in aqueous buffer

112   Blocking experiments were performed to be absolutely sure that the vimentin Cys was the
113   reactive group for coupling to MHI-148 in aqueous buffer at 37 °C.   Thus, maleimide-blocked
114   protein [24,25] was formed by incubating vimentin with 6-maleimidohexanoic acid (6-MA; 18 h in
115   50 mM pH 7.24 HEPES buffer at 37 °C).   Vimentin and the thiol-blocked vimentin were incubated
116   with MHI-148 for different incubation times, then analyzed using SDS-PAGE gel electrophoresis.
117   Figure 4c shows the concentration of MHI-148 covalently bound to vimentin progressively
118   increased (NIR fluorescence at ~800 nm) whereas no fluorescent band was observed for the
119   thiol-blocked vimentin.

(a)   (b)

(c)
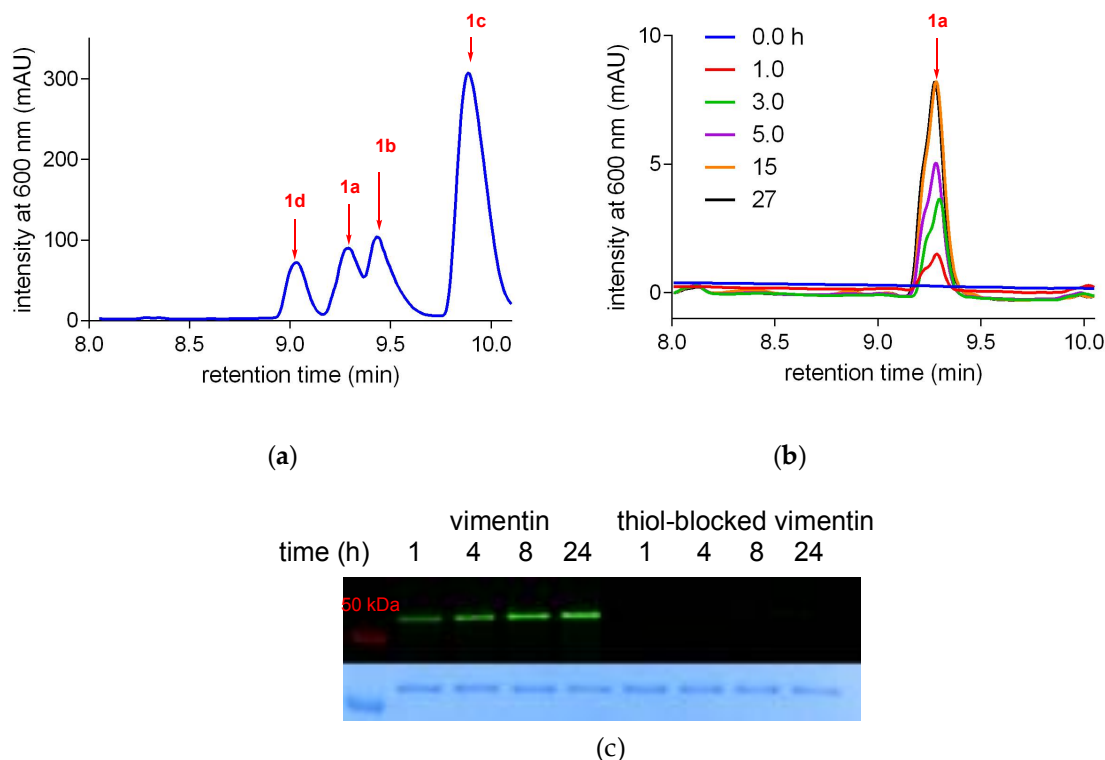
Figure 4. HPLC analysis of (**a**) 200 µM of each amino acid-conjugate standards **1a-d** in 50 mM pH 8.0 HEPES buffer; (**b**) kinetic study for 200 µM of MHI148 with 200 µM of each amino acid (*N*-acetyl-L-Cys, *N*-acetyl-L-Tyr, *N*α-acetyl-L-Lys, *N*ε-acetyl-L-Lys, and L-proline) in 50 mM pH 8.0 HEPES buffer incubating at 37 °C; (**c**) NIR-fluorescent gel image of vimentin or 6-MA-blocked vimentin (1 µM) incubated with MHI-148 (1 µM) in 50 mM pH 7.24 HEPES buffer at different incubation time

Overall, based on all the experiments above, we concluded MHI-148 selectively binds the only free Cys in vimentin, C328, in aqueous buffer at 37 °C, and went on to calibrate the efficiency of binding.   Thus, NIR fluorescence (> 800 nm) in gel electrophoresis was qualitative for vimentin (1 µM in 50 mM pH 7.24 HEPES buffer) when incubated with of MHI-148 (0 to 30 µM, 3 h at 37 °C). Fluorescence intensities of the salient band saturated at 10 µM (Figure 5a), which means the tested fluorescent compound can qualitatively label the protein at 10:1 ratio within 3 h when incubated under these conditions in HEPES aqueous buffer.   Experiments to test sensitivity revealed labeled vimentin was detectable at concentrations as low as 1 ng on our gel imaging apparatus (Figure 5b).

(a)   (b)
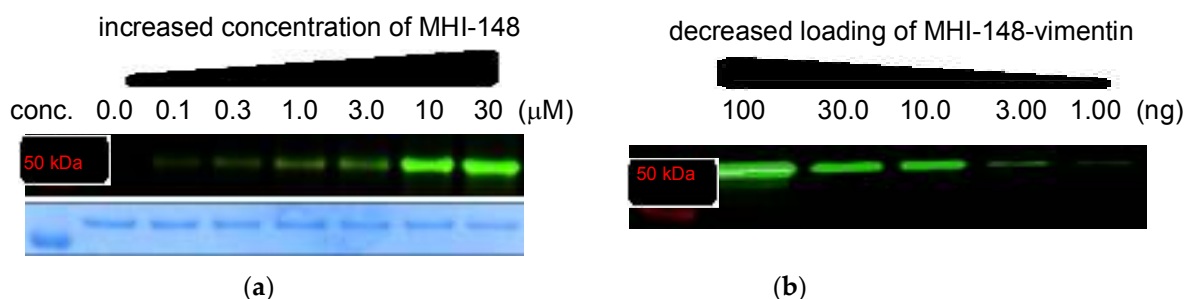
Figure 5. NIR-fluorescent gel image of (**a**) vimentin (1 µM) incubated with different concentrations of MHI-148 in 50 mM pH 7.24 HEPES buffer for 3 h at 37 °C (**b**) 10:1 concentration ratio of MHI-148:vimentin sample was loaded into 10% SDS-PAGE gel with different amount of vimentin sample

146   *2.4. Labeling Of Other Proteins Using MHI-148*

147   Several proteins with and without free Cys residues were labeled to test the robustness of the
148   method developed for vimentin. NEDD8-activating enzyme (NAE) [26], Ubc12 [27], and PCSK9 [28]
149   contain free thiols (reduced Cys residues) whereas NEDD8 [26] (no Cys in sequences), truncated
150   suPAR (residues 1-281, 12 disulfides) [29], and EGFR (25 disulfides) [30] have none.   Figure 6 shows
151   that only the proteins containing sulfhydryl groups reacted under the standard conditions.   NAE
152   consists of two subunits (APPBP1 and UBA3), that each contains free Cys hence two NIR
153   fluorescence bands were observed for that sample.

154

155   **Figure 6.** NIR-fluorescent gel image of diverse proteins (4 μM) incubated with MHI-148 (4 μM) for 3
156   h using 50 mM pH 7.24 HEPES buffer at 37 °C

157   **3. Conclusions**

158   MHI-148 can generally label proteins containing free Cys residues with some generality.
159   Other Cy-7 dyes containing *meso*-Cl were only used to label vimentin in this work, but it would be
160   unsurprising if they can be used.   It seems clear that this methodology could be applied with a high
161   probability of success to conveniently conjugate *meso*-Cl near-IR dyes to antibodies, monobodies,
162   and nanobodies to form selective agents for optical imaging *in vivo*.   Traditional conjugation
163   techniques tend to require modification of the dye to include maleimide or succinimide functionality
164   [25,31,32], but the method developed here circumvents that process.

165   **4. Materials and Methods**

166   *4.1. General Information*

167   All reactions were carried out with dry solvents under anhydrous conditions under an inert
168   atmosphere (argon). Glassware was dried in an oven at 140 °C for a minimum of 6 h prior to use for
169   all reactions. IR-783 and IR-780 was purchased from Sigma Aldrich and abcr GmBH respectively,
170   DZ-1 and MHI-148 were synthesized according to literature protocol [7,12,14].   All other reagents
171   were purchased at a high commercial quality (typically 97 % or higher) and used without further
172   purification, unless otherwise stated.   Products were purified using a reverse-phase column on a
173   preparation high performance liquid chromatography (prep HPLC) obtained from solid-phase
174   synthesis in 10-95% MeCN/water with 0.05 % trifluoroacetic acid over 20 minutes. High-field NMR
175   spectra were recorded with Bruker Avance III at 400 MHz for ^{1}H, and 100 MHz for ^{13}C for all
176   compounds. All spectra were calibrated using residual non-deuterated solvent as an internal
177   reference (MeOD-d$_4$: ^{1}H NMR = 3.30, ^{13}C NMR = 49.0, DMSO-d$_6$: ^{1}H NMR = 2.50, ^{13}C NMR = 39.5).
178   The following abbreviations were used to explain the multiplicities: s = singlet, d = doublet, t =

179   triplet, q = quartet, quint = quintet, dd = double doublet, dt = double triplet, dq = double quartet, m =
180   multiplet.   Electrospray ionization mass spectrometry (ESI-MS) data were collected on triple-stage
181   quadrupole instrument in a positive mode.   All statistical analyses were carried out by GraphPad
182   Prism version 6.0 (GraphPad Software).

183   *4.2. Synthesis And Characterization*

184   4.2.1. 2-((*E*)-2-((*E*)-2-(((*R*)-2-acetamido-2-carboxyethyl)thio)-3-(2-((*E*)-1-(5-carboxypentyl)-3,3-
185   dimethylindolin-2-ylidene)ethylidene)cyclohex-1-en-1-yl)vinyl)-1-(5-carboxypentyl)-3,3-dimethyl-3
186   *H*-indol-1-ium (**1a**)

187   To a solution of MHI-148 (25.0 mg, 0.04 mmol) in DMF (1.00 mL), *N*-acetyl-L-cysteine (5.98 mg, 0.04
188   mmol), and ^{i}Pr$_2$NEt (9.41 μL, 0.06 mmol) were added and the reaction was stirred at 25 °C for 1 h.
189   Solvent was removed under a stream of nitrogen gas and purified by preparative reversed-phase
190   HPLC (10% - 95% CH$_3$CN/water containing 0.05% TFA).   Compound was lyophilized to obtain
191   green solid (23.4 mg, 78%). ^{1}H NMR (400 MHz, MeOD) δ 8.77 (d, *J* = 13.9 Hz, 2H), 7.49 (d, *J* = 7.3 Hz,
192   2H), 7.45 – 7.36 (m, 2H), 7.27 (dd, *J* = 14.9, 7.6 Hz, 4H), 6.28 (d, *J* = 13.8 Hz, 2H), 4.55 (dd, *J* = 7.5, 5.3 Hz,
193   1H), 4.15 (t, *J* = 6.9 Hz, 4H), 3.40 (dd, *J* = 13.4, 5.3 Hz, 1H), 3.12 (dd, *J* = 13.4, 7.5 Hz, 1H), 2.75 – 2.54 (m,
194   4H), 2.31 (t, *J* = 7.3 Hz, 4H), 1.98 – 1.92 (m, 2H), 1.95 (s, 3H), 1.90 – 1.80 (m, 4H), 1.74 (s, 12H), 1.72 –
195   1.64 (m, 4H), 1.55 – 1.45 (m, 4H). ^{13}C NMR (100 MHz, MeOD) δ 177.23, 173.86, 173.21, 172.93, 157.83,
196   146.46, 143.72, 142.48, 134.54, 129.83, 126.27, 123.46, 112.00, 102.20, 54.36, 50.51, 50.49, 49.85, 44.97,
197   39.51, 34.61, 28.44, 28.02, 27.38, 25.65, 22.75, 22.03. HRMS calculated for C$_{47}$H$_{60}$N$_3$O$_7$S$^+$ (M)$^+$: 810.4146;
198   found 810.4166

199   4.2.2. 6-((*E*)-2-((*E*)-2-(2-(4-(2-acetamido-2-carboxyethyl)phenoxy)-3-((*E*)-2-(1-(5-carboxypentyl)-3,3-
200   dimethyl-3*H*-indol-1-ium-2-yl)vinyl)cyclohex-2-en-1-ylidene)ethylidene)-3,3-dimethylindolin-1-yl)h
201   exanoate (**1b**)

202   NaH (0.89 mg, 0.04 mmol) was added into a solution of *N*-acetyl-L-tyrosine (8.25 mg, 0.04 mmol) in
203   DMF (1.00 mL) and the reaction was stirred at 25 °C for 30 min.   MHI-148 (25.0 mg, 0.04 mmol)
204   was then added to the above reaction and the reaction was stirred for an additional 18 h at 25 °C.
205   Solvent was removed under a stream of nitrogen gas and purified by preparative reversed-phase
206   HPLC (10% - 95% CH$_3$CN/water containing 0.05% TFA).   Compound was lyophilized to obtain
207   green solid (12.2 mg, 38%). ^{1}H NMR (400 MHz, MeOD) δ 8.01 – 7.92 (m, 2H), 7.36 (t, *J* = 7.8 Hz, 4H),
208   7.31 – 7.15 (m, 6H), 7.05 (d, *J* = 8.7 Hz, 2H), 6.13 (d, *J* = 14.2 Hz, 2H), 4.54 (dd, *J* = 9.1, 5.2 Hz, 1H), 4.09
209   (t, *J* = 7.3 Hz, 4H), 3.14 (dd, *J* = 14.0, 5.2 Hz, 1H), 2.84 (dd, *J* = 14.2, 9.2 Hz, 1H), 2.73 (t, *J* = 5.8 Hz, 4H),
210   2.30 (t, *J* = 7.3 Hz, 4H), 2.04 (t, *J* = 7.3 Hz, 2H), 1.84 (s, 3H), 1.83 – 1.73 (m, 4H), 1.67 (dd, *J* = 15.1, 7.5 Hz,
211   4H), 1.46 (t, *J* = 7.7 Hz, 4H), 1.33 (s, 12H). ^{13}C NMR (100 MHz, MeOD) δ 177.20, 174.59, 173.75, 173.05,
212   165.43, 160.25, 143.57, 143.34, 142.51, 132.96, 132.16, 129.76, 126.19, 123.40, 123.20, 115.75, 111.94,
213   100.93, 55.48, 50.27, 44.85, 37.62, 34.59, 28.25, 27.96, 27.33, 25.63, 25.21, 22.48, 22.39. HRMS calculated
214   for C$_{53}$H$_{64}$N$_3$O$_8$$^+$ (M)$^+$: 870.4688; found 870.4675

215   4.2.3. 1-(5-carboxypentyl)-2-((*E*)-2-((*E*)-3-(2-((*E*)-1-(5-carboxypentyl)-3,3-dimethylindolin-2-ylidene)
216   ethylidene)-2-((*S*)-2-carboxypyrrolidin-1-yl)cyclohex-1-en-1-yl)vinyl)-3,3-dimethyl-3*H*-indol-1-ium
217   (**1c**)

218   To a solution of MHI-148 (25.0 mg, 0.04 mmol) in DMF (1.00 mL), L-proline (4.26 mg, 0.04 mmol),
219   and ^{i}Pr$_2$NEt (6.27 μL, 0.04 mmol) were added and the reaction was stirred at 60 °C monitored by
220   Agilent LC-MS.   The reaction was reached equilibrium after 2 h and the solvent was removed
221   under a stream of nitrogen gas and purified by preparative reversed-phase HPLC (10% - 95%
222   CH$_3$CN/water containing 0.05% TFA). Compound was lyophilized to obtain blue solid (5.18 mg,
223   18%). ^{1}H NMR (400 MHz, DMSO) δ 7.42 (d, *J* = 7.3 Hz, 2H), 7.28 (t, *J* = 7.7 Hz, 2H), 7.11 (d, *J* = 7.7 Hz,
224   2H), 7.04 (t, *J* = 7.2 Hz, 2H), 5.68 (d, *J* = 12.4 Hz, 2H), 4.96 (d, *J* = 7.3 Hz, 2H), 4.02 – 3.97 (m, 1H), 3.90 –

225 3.87 (m, 4H), 2.76 – 2.57 (m, 3H), 2.46 – 2.29 (m, 3H), 2.28 – 2.18 (m, 1H), 2.20 (t, J = 7.3 Hz, 4H), 2.09 –
226 1.98 (m, 3H), 1.79 – 1.70 (m, 2H), 1.70 – 1.62 (m, 4H), 1.57 (s, 6H), 1.61 – 1.48 (m, 4H), 1.54 (s, 6H), 1.45
227 – 1.30 (m, 4H). ^{13}C NMR (100 MHz, DMSO) δ 174.29, 172.71, 166.02, 158.00, 142.99, 139.74, 136.52,
228 128.11, 123.13, 122.28, 122.00, 109.00, 94.22, 64.69, 56.49, 46.93, 42.26, 33.52, 30.04, 29.59, 28.65, 28.11,
229 26.70, 25.81, 24.22, 20.65. HRMS calculated for $C_{47}H_{60}N_3O_6^+$ (M)$^+$: 762.4477; found 762.4457

230 4.2.4. 2-((*E*)-2-((*E*)-2-(((*S*)-5-acetamido-1-carboxypentyl)amino)-3-(2-((*E*)-1-(5-carboxypentyl)-3,3-
231 dimethylindolin-2-ylidene)ethylidene)cyclohex-1-en-1-yl)vinyl)-1-(5-carboxypentyl)-3,3-dimethyl-3
232 *H*-indol-1-ium (**1d**)

233 To a solution of MHI-148 (25.0 mg, 0.04 mmol) in DMF/H$_2$O (1:1; 1.00 mL), Nε-acetyl-L-lysine (6.96
234 mg, 0.04 mmol), and ^{i}Pr$_2$NEt (6.27 μL, 0.04 mmol) were added and the reaction was stirred at 60 °C
235 monitored by Agilent LC-MS.   The reaction was reached equilibrium after 20 h and the solvent
236 was removed under a stream of nitrogen gas and purified by preparative reversed-phase HPLC (10%
237 - 95% CH$_3$CN/water containing 0.05% TFA). Compound was lyophilized to obtain blue solid (4.33
238 mg, 18%). ^{1}H NMR (400 MHz, DMSO) δ 8.02 (d, J = 9.4 Hz, 1H), 7.78 (d, J = 12.9 Hz, 2H), 7.45 (d, J =
239 7.2 Hz, 2H), 7.35 – 7.28 (m, 2H), 7.24 (dd, J = 11.6, 3.9 Hz, 1H), 7.17 (d, J = 8.0 Hz, 2H), 7.09 (t, J = 7.4
240 Hz, 2H), 7.05 – 7.00 (m, 1H), 5.85 (d, J = 13.2 Hz, 2H), 4.43 (dd, J = 13.9, 8.8 Hz, 1H), 4.00 – 3.95 (m,
241 4jH), 3.68 – 3.61 (m, 4H), 3.01 (t, J = 5.4 Hz, 2H), 2.56 (dd, J = 13.9, 7.2 Hz, 2H), 2.42 – 2.33 (m, 2H), 2.20
242 (dd, J = 13.4, 6.3 Hz, 4H), 1.75 (s, 3H), 1.72 – 1.63 (m, 6H), 1.60 (s, 12H), 1.52 (dd, J = 14.8, 7.4 Hz, 6H),
243 1.43 – 1.34 (m, 8H). ^{13}C NMR (100 MHz, DMSO) δ 174.22, 173.25, 168.88, 167.91, 142.71, 140.05, 128.12,
244 127.58, 122.74, 122.42, 121.96, 120.58, 109.39, 108.49, 95.36, 47.32, 43.24, 42.35, 38.21, 33.47, 28.99, 28.01,
245 27.60, 25.94, 25.77, 25.62, 24.45, 24.18, 24.11, 24.05, 22.53. HRMS calculated for $C_{50}H_{67}N_4O_7^+$ (M)$^+$:
246 835.5004; found 835.4972

247 *4.3. UV-Vis And Fluorescence Analysis*

248   6 μM of compounds **1a-d** samples in 10 mM PBS buffer was prepared by diluting their
249 corresponding stock solution (20 mM) in DMSO using pH 7.24 10 mM PBS buffer.   The absorbance
250 and fluorescence of these samples were analyzed using Varian Cary 100 UV-Vis Spectrometer and
251 Varian Cary Eclipse Fluorescence Spectrophotometer, respectively. The normalized absorbance and
252 fluorescence data were plotted using GraphPad Prism version 6.0 (GraphPad Software).

253 *4.4. NIR Gel Image Protocol*

254   Different cyanines (10 μM; 20 mM stock in DMSO) were incubated with vimentin (1 μM; 1 μg)
255 in pH 7.24 HEPES buffer (50 mM) at 37 °C monitored up to 24 h. 100 ng of each cyanine-vimentin
256 conjugate samples were treated under reducing condition with heating at 95 °C for 10 min and
257 loaded into 15 % SDS-PAGE for electrophoresis.   The gel was washed with de-ionized water (10
258 min × 3 times), and the gel was analyzed by an Odyssey imager to detect the Near IR fluorescence

259 *4.5. Preparation of Thiol-blocked Vimentin*

260   Using pH 7.24 HEPES buffer (50 mM), thiol-blocked vimentin was prepared by incubating
261 6-maleimide-hexanoic acid (6-MA, 10 μM) with vimentin (1 μg, 1 μM) for 18 h at 37 °C.   The
262 thiol-blocked vimentin solution was directly used to incubate with MHI-148 (1 μM) without further
263 purifications.

264 *4.6. Kinetic Study Of MHI-148 With Amino Acids In Aqueous Buffer*

265   To a solution of MHI-148 (400 μM) in pH 8.00 HEPES buffer (500 μL), 100 μL of each amino acid
266 solution (2.00 mM) in pH 8.00 HEPES buffer was added to make a final concentration of 200 μM of
267 each reagent. The reaction was incubated and shaken at 37 °C, and was monitored using HPLC at
268 600 nm from 0 to 27 h at which reached reaction equilibrium.   The data was plotted using
269 GraphPad Prism version 6.0 (GraphPad Software).

270   *4.7. NIR Gel Image Of MHI-148 With Different Proteins*

271   Different proteins including NEDD8, Ubc12, truncated suPAR (residues 1-281), NAE, PCSK9,
272   EGFR (4 μM; 1 μg) were incubated with MHI-148 (4 μM) in pH 7.24 HEPES buffer (50 mM) at 37 °C
273   for 3 h. 500 ng of each protein samples were treated under non-reducing condition with heating at 95
274   °C for 10 min and loaded into 10 % SDS-PAGE for electrophoresis. The gel was washed with
275   deionized water (10 min × 3 times), and the gel was analyzed by an Odyssey imager to detect the
276   Near-IR fluorescence

289
290   **References**

291   1.   Shi, C.; Wu Jason, B.; Pan, D. Review on near-infrared heptamethine cyanine dyes as
292   theranostic agents for tumor imaging, targeting, and photodynamic therapy. *J. Biomed. Opt.*
293   **2016**, *21*, 50901:1-50901:11, doi: 10.1117/1.JBO.21.5.050901.

294   2.   Schaafsma, B.E.; Mieog, J.S.D.; Hutteman, M.; van der Vorst, J.R.; Kuppen, P.J.K.; Loewik,
295   C.W.G.M.; Frangioni, J.V.; van de Velde, C.J.H.; Vahrmeijer, A.L. The clinical use of
296   indocyanine green as a near-infrared fluorescent contrast agent for image-guided oncologic
297   surgery. *J. Surg. Oncol.* **2011**, *104*, 323-332, doi:10.1002/jso.21943.

298   3.   Alander, J.T.; Kaartinen, I.; Laakso, A.; Patila, T.; Spillmann, T.; Tuchin, V.V.; Venermo, M.;
299   Valisuo, P. A review of indocyanine green fluorescent imaging in surgery. *Int. J. Biomed.*
300   *Imaging* **2012**, 940585:1-940585:26, doi:10.1155/2012/940585.

301   4.   Nagahara, R.; Onda, N.; Yamashita, S.; Kojima, M.; Inohana, M.; Eguchi, A.; Nakamura, M.;
302   Matsumoto, S.; Yoshida, T.; Shibutani, M. Fluorescence tumor imaging by i.v. administered
303   indocyanine green in a mouse model of colitis-associated colon cancer. *Cancer Sci.* **2018**, *109*,
304   1638-1647, doi:10.1111/cas.13564.

305   5.   Luo, S.; Zhang, E.; Su, Y.; Cheng, T.; Shi, C. A review of NIR dyes in cancer targeting and
306   imaging. *Biomaterials* **2011**, *32*, 7127-7138, doi:10.1016/j.biomaterials.2011.06.024.

307   6.   James, N.S.; Chen, Y.; Joshi, P.; Ohulchanskyy, T.Y.; Ethirajan, M.; Henary, M.; Strekowski,
308   L.; Pandey, R.K. Evaluation of polymethine dyes as potential probes for near infrared
309   fluorescence imaging of tumors: part - 1. *Theranostics* **2013**, *3*, 692-702, doi:10.7150/thno.5922.

310   7.   Yang, X.; Shi, C.; Tong, R.; Qian, W.; Zhau, H.E.; Wang, R.; Zhu, G.; Cheng, J.; Yang, V.W.;
311   Cheng, T., et al. Near IR Heptamethine Cyanine Dye-Mediated Cancer Imaging. *Clin. Cancer*
312   *Res.* **2010**, *16*, 2833-2844, doi:10.1158/1078-0432.ccr-10-0059.

313   8.   Henary, M.; Pannu, V.; Owens, E.A.; Aneja, R. Near infrared active heptacyanine dyes with
314   unique cancer-imaging and cytotoxic properties. *Bioorg. Med. Chem. Lett.* **2012**, *22*, 1242-1246,
315   doi:10.1016/j.bmcl.2011.11.070.
316   9.   Yuan, J.; Yi, X.; Yan, F.; Wang, F.; Qin, W.; Wu, G.; Yang, X.; Shao, C.; Chung, L.W.K.
317   Near-Infrared Fluorescence Imaging of Prostate Cancer Using Heptamethine Carbocyanine
318   Dyes. *Mol. Med. Rep.* **2015**, *11*, 821-828, doi:10.3892/mmr.2014.2815.
319   10.   Zhao, N.; Zhang, C.; Zhao, Y.; Bai, B.; An, J.; Zhang, H.; Shi, C.; Wu Jason, B. Optical Imaging
320   of Gastric Cancer With Near-Infrared Heptamethine Carbocyanine Fluorescence Dyes.
321   *Oncotarget* **2016**, *7*, 57277-57289.
322   11.   Yang, X.; Shao, C.; Wang, R.; Chu, C.-Y.; Hu, P.; Master, V.; Osunkoya, A.O.; Kim, H.L.;
323   Zhau, H.E.; Chung, L.W.K. Optical Imaging of Kidney Cancer with Novel Near Infrared
324   Heptamethine Carbocyanine Fluorescent Dyes. *J. Urol.* **2013**, *189*, 702-710,
325   doi:10.1016/j.juro.2012.09.056.
326   12.   Zhang, C.; Zhao, Y.; Zhang, H.; Chen, X.; Zhao, N.; Tan, D.; Zhang, H.; Shi, C. The
327   Application of Heptamethine Cyanine Dye DZ-1 and Indocyanine Green for Imaging and
328   Targeting in Xenograft Models of Hepatocellular Carcinoma. *Int. J. Mol. Sci.* **2017**, *18*.
329   13.   Wu, J.B.; Lin, T.-P.; Gallagher, J.D.; Kushal, S.; Chung, L.W.K.; Zhau, H.E.; Olenyuk, B.Z.;
330   Shih, J.C. Monoamine Oxidase A Inhibitor-Near-Infrared Dye Conjugate Reduces Prostate
331   Tumor Growth. *J. Am. Chem. Soc.* **2015**, *137*, 2366-2374, doi:10.1021/ja512613j.
332   14.   Wu, J.B.; Shi, C.; Chu, G.C.-Y.; Xu, Q.; Zhang, Y.; Li, Q.; Yu, J.S.; Zhau, H.E.; Chung, L.W.K.
333   Near-Infrared Fluorescence Heptamethine Carbocyanine Dyes Mediate Imaging and
334   Targeted Drug Delivery for Human Brain Tumor. *Biomaterials* **2015**, *67*, 1-10,
335   doi:10.1016/j.biomaterials.2015.07.028.
336   15.   Guan, Y.; Zhang, Y.; Xiao, L.; Li, J.; Wang, J.-p.; Chordia, M.D.; Liu, Z.-Q.; Chung, L.W.K.;
337   Yue, W.; Pan, D. Improving Therapeutic Potential of Farnesylthiosalicylic Acid: Tumor
338   Specific Delivery via Conjugation with Heptamethine Cyanine Dye. *Mol. Pharmaceutics* **2017**,
339   *14*, 1-13, doi:10.1021/acs.molpharmaceut.5b00906.
340   16.   Lv, Q.; Yang, X.; Wang, M.; Yang, J.; Qin, Z.; Kan, Q.; Zhang, H.; Wang, Y.; Wang, D.; He, Z.
341   Mitochondria-targeted prostate cancer therapy using a near-infrared fluorescence
342   dye-monoamine oxidase A inhibitor conjugate. *J. Controlled Release* **2018**, *279*, 234-242,
343   doi:10.1016/j.jconrel.2018.04.038.
344   17.   Strekowski, L.; Lipowska, M.; Patonay, G. Facile derivatizations of heptamethine cyanine
345   dyes. *Synth. Commun.* **1992**, *22*, 2593-2598, doi:10.1080/00397919208021656.
346   18.   Strekowski, L.; Lipowska, M.; Patonay, G. Substitution reactions of a nucleofugal group in
347   heptamethine cyanine dyes. Synthesis of an isothiocyanato derivative for labeling of
348   proteins with a near-infrared chromophore. *J. Org. Chem.* **1992**, *57*, 4578-4580,
349   doi:10.1021/jo00043a009.
350   19.   Cha, J.; Nani, R.R.; Luciano, M.P.; Broch, A.; Kim, K.; Namgoong, J.-M.; Kulkarni, R.A.;
351   Meier, J.L.; Kim, P.; Schnermann, M.J. A chemically stable fluorescent marker of the ureter.
352   *Bioorg. Med. Chem. Lett.* **2018**, *28*, 2741-2745, doi:10.1016/j.bmcl.2018.02.040.
353   20.   Nani, R.R.; Shaum, J.B.; Gorka, A.P.; Schnermann, M.J. Electrophile-Integrating Smiles
354   Rearrangement Provides Previously Inaccessible C4'-O-Alkyl Heptamethine Cyanine
355   Fluorophores. *Org. Lett.* **2015**, *17*, 302-305, doi:10.1021/ol503398f.

356 21. Guo, Z.; Zhu, W.; Zhu, M.; Wu, X.; Tian, H. Near-Infrared Cell-Permeable Hg2+-Selective
357   Ratiometric Fluorescent Chemodosimeters and Fast Indicator Paper for MeHg+ Based on
358   Tricarbocyanines. *Chem. - Eur. J.* **2010**, *16*, 14424-14432, doi:10.1002/chem.201001769.

359 22. Njiojob, C.N.; Owens, E.A.; Narayana, L.; Hyun, H.; Choi, H.S.; Henary, M. Tailored
360   Near-Infrared Contrast Agents for Image Guided Surgery. *J. Med. Chem.* **2015**, *58*, 2845-2854,
361   doi:10.1021/acs.jmedchem.5b00253.

362 23. Peng, X.; Song, F.; Lu, E.; Wang, Y.; Zhou, W.; Fan, J.; Gao, Y. Heptamethine cyanine dyes
363   with a large stokes shift and strong fluorescence: a paradigm for excited-state intramolecular
364   charge transfer. *J. Am. Chem. Soc.* **2005**, *127*, 4170-4171, doi:10.1021/ja043413z.

365 24. Warnecke, A.; Fichtner, I.; Garmann, D.; Jaehde, U.; Kratz, F. Synthesis and Biological
366   Activity of Water-Soluble Maleimide Derivatives of the Anticancer Drug Carboplatin
367   Designed as Albumin-Binding Prodrugs. *Bioconjugate Chem.* **2004**, *15*, 1349-1359,
368   doi:10.1021/bc049829j.

369 25. Nanda, J.S.; Lorsch, J.R. Labeling of a protein with fluorophores using maleimide
370   derivitization. *Methods Enzymol.* 536; Lorsch, J., Ed., Elsevier: San Diego, CA, **2014**, pp. 79-86.
371   ISBN 978-0-12-420070-8.

372 26. Walden, H.; Podgorski, M.S.; Huang, D.T.; Miller, D.W.; Howard, R.J.; Minor, D.L., Jr.;
373   Holton, J.M.; Schulman, B.A. The structure of the APPBP1-UBA3-NEDD8-ATP complex
374   reveals the basis for selective ubiquitin-like protein activation by an E1. *Mol. Cell* **2003**, *12*,
375   1427-1437, doi:10.1016/s1097-2765(03)00452-0.

376 27. Huang, D.T.; Miller, D.W.; Mathew, R.; Cassell, R.; Holton, J.M.; Roussel, M.F.; Schulman,
377   B.A. A unique E1-E2 interaction required for optimal conjugation of the ubiquitin-like
378   protein NEDD8. *Nat. Struct. Mol. Biol.* **2004**, *11*, 927-935, doi:10.1038/nsmb826.

379 28. Cunningham, D.; Danley, D.E.; Geoghegan, K.F.; Griffor, M.C.; Hawkins, J.L.; Subashi, T.A.;
380   Varghese, A.H.; Ammirati, M.J.; Culp, J.S.; Hoth, L.R., et al. Structural and biophysical
381   studies of PCSK9 and its mutants linked to familial hypercholesterolemia. *Nat. Struct. Mol.*
382   *Biol.* **2007**, *14*, 413-419, doi:10.1038/nsmb1235.

383 29. Llinas, P.; Le Du, M.H.; Gardsvoll, H.; Dano, K.; Ploug, M.; Gilquin, B.; Stura, E.A.; Menez,
384   A. Crystal structure of the human urokinase plasminogen activator receptor bound to an
385   antagonist peptide. *Embo J.* **2005**, *24*, 1655-1663, doi:10.1038/sj.emboj.7600635.

386 30. Ogiso, H.; Ishitani, R.; Nureki, O.; Fukai, S.; Yamanaka, M.; Kim, J.-H.; Saito, K.; Sakamoto,
387   A.; Inoue, M.; Shirouzu, M., et al. Crystal structure of the complex of human epidermal
388   growth factor and receptor extracellular domains. *Cell* **2002**, *110*, 775-787.

389 31. Sato, K.; Gorka, A.P.; Nagaya, T.; Michie, M.S.; Nakamura, Y.; Nani, R.R.; Coble, V.L.;
390   Vasalatiy, O.V.; Swenson, R.E.; Choyke, P.L., et al. Effect of charge localization on the in vivo
391   optical imaging properties of near-infrared cyanine dye/monoclonal antibody conjugates.
392   *Mol. BioSyst.* **2016**, *12*, 3046-3056, doi:10.1039/c6mb00371k.

393 32. Nani, R.R.; Gorka, A.P.; Nagaya, T.; Kobayashi, H.; Schnermann, M.J. Near-IR
394   Light-Mediated Cleavage of Antibody-Drug Conjugates Using Cyanine Photocages. *Angew.*
395   *Chem., Int. Ed.* **2015**, *54*, 13635-13638, doi:10.1002/anie.201507391.

396
397
398